Nuclear Engineering and Technology 55 (2023) 1924–1934

Contents lists available at ScienceDirect

Nuclear Engineering and Technology

journal homepage: www.elsevier.com/locate/net

Original Article

Statistical analysis of S–N type environmental fatigue data of Ni-base alloy welds using weibull distribution

Jae Phil Park [a], Junhyuk Ham [b], Subhasish Mohanty [c], Dayu Fajrul Falaakh [a], Ji Hyun Kim [b], Chi Bum Bahn [a,*]

[a] School of Mechanical Engineering, Pusan National University, Busan, 46241, Republic of Korea
[b] Department of Nuclear Engineering, Ulsan National Institute of Science and Technology, Ulsan, 44919, Republic of Korea
[c] Nuclear Science and Engineering, Argonne National Laboratory, Lemont, IL, 60439, USA

A R T I C L E I N F O

Article history:
Received 2 March 2022
Received in revised form
8 August 2022
Accepted 8 August 2022
Available online 16 August 2022

Keywords:
Environmental fatigue
Ni-base alloy weld
S-N curve
Statistical analysis
Weibull distribution

A B S T R A C T

In this study, the probabilistic fatigue life model for Ni-base alloys was developed based on the Weibull distribution using statistical analysis of fatigue data reported in NUREG/CR-6909 and the new fatigue data of Alloy 52M/152 and 82/182. The developed Weibull model can consider right-censored data (i.e., non-failed data) and quantify the improved safety (or reliability) based on the level of failure probability. The overall margin in the current fatigue design limit model (ASME design curve + NUREG/CR-6909 F_{en} model) is similar to that of the Weibull model with a cumulative failure probability of approximately 2.5%. The margin in the current fatigue design limit model demonstrated inconsistencies for the Ni-base alloy weld data, whereas the Weibull model showed a consistent margin. Therefore, the Weibull model can systematically mitigate the excessive safety margin.

1. Introduction

The metallic components of pressure boundaries in nuclear power plants (NPPs) can gradually degrade due to cyclic loading (i.e., fatigue), even below the designed static loads [1]. Fatigue on the pressure boundary components of NPPs can occur for various reasons, such as shutdown/restart, flow-induced vibration, and thermal shock [2]. Therefore, the structural integrity of the component needs to be guaranteed from the design stage of NPPs. This is by comparing postulated fatigue cycles with fatigue design limits (or fatigue design curves), as specified in the American Society of Mechanical Engineers (ASME) Boiler & Pressure Vessel Code Section III [1,3]. The ASME fatigue design curve is based on the best-fitting curve of the in-air fatigue life data for a given stress/strain amplitude, and then corrected to consider the associated uncertainties (e.g., surface finish, material grade, etc.).

In pressurized water reactor (PWR) coolant systems of NPPs, Ni-base dissimilar metal welds (DMWs) are widely used to join low-alloy steel components (e.g., reactor pressure vessels, steam generators, reactor coolant pump casings, and pressurizers) to stainless steel piping or nozzles [4]. However, in practice, the Ni-base DMW joint is one of the most vulnerable locations in the PWR pressure boundaries. This is due to the residual stress formed during the welding process, different material properties (at the interface of various materials) and their interaction with the reactor cyclic loading and coolant environment [5]. For Ni-base alloys and their weldments, the ASME code ensures the fatigue design curve of Ni-base alloys to follow the fatigue design curve of austenitic stainless steel (AuSS) [1,3]. The fatigue design curve of AuSS is determined using an adjustment life factor of 12 and a stress/strain factor of 2 based on the best-fit in-air S–N (stress/strain amplitude vs. fatigue life) curve of AuSS (i.e., Eq. 1):

$$\ln N_{f,\,\mathrm{Air}} = 6.891 - 1.920\,\ln(\varepsilon_a - 0.112) \tag{1}$$

where $N_{f,\,\mathrm{Air}}$ is the in-air fatigue life (number of cycles), and ε_a is the strain amplitude (%).

However, there is a limitation that the fatigue design curve mentioned above was developed based on only in-air fatigue test data. Laboratory data have reported that the environmental effect of corrosion considerably shortens the fatigue life [6–14]. For

* Corresponding author.
E-mail address: bahn@pusan.ac.kr (C.B. Bahn).

https://doi.org/10.1016/j.net.2022.08.005

example, the Nuclear Regulatory Commission (NRC) report NUREG/CR-6909 [1], a technical background document of Reg. Guide 1.207 [15] reported that the fatigue life is shortened by 12 times for AuSS, 3 times for NiCrFe alloys, and approximately 17 times for carbon steels in a light water reactor (LWR) coolant environment. Thus, Reg. Guide 1.207 required the fatigue design curve to be corrected by multiplying an additional environmental correction factor to account for these environmental effects in the LWR coolant system. In NUREG/CR-6909, the environmental correction factor model for Ni-base alloys, except for Alloy 718, was presented as a function of temperature, strain rate, and dissolved oxygen (DO) as follows [1]:

- Definition of environmental correction factor:

$$F_{\mathrm{en}} = \frac{N_{f,\mathrm{air}}}{N_{f,\ \mathrm{water}}} \tag{2}$$

- Calculation of environmental correction factor (for Ni-base alloys):

$$F_{\mathrm{en}} = \exp(-T^{*}\dot{\varepsilon}^{*}O^{*}) \tag{3a}$$

$$T^{*} = \begin{cases} 0 & (T < 50^{\circ}C) \\ \dfrac{T-50}{275} & (50^{\circ}C \le T \le 325^{\circ}C) \end{cases} \tag{3b}$$

$$\dot{\varepsilon}^{*} = \begin{cases} 0 & (\dot{\varepsilon} > 5.0\%/s) \\ \ln\dfrac{\dot{\varepsilon}}{5} & (0.0004\ \%/s \le \dot{\varepsilon} \le 5.0\ \%/s) \\ \ln\dfrac{0.0004}{5} & (\dot{\varepsilon} < 0.0004\ \%/s) \end{cases} \tag{3c}$$

$$O^{*} = \begin{cases} 0.06 & (\text{NWC BWR water},\ \text{DO} \ge 0.1\ \text{ppm}) \\ 0.14 & (\text{PWR or HWC BWR water},\ \text{DO} < 0.1\ \text{ppm}) \end{cases} \tag{3d}$$

where F_{en} is the environmental correction factor, $N_{f,\mathrm{water}}$ is the LWR-water fatigue life, T is the temperature (°C), $\dot{\varepsilon}$ is the strain rate (%/s), and T^{*}, $\dot{\varepsilon}^{*}$, and O^{*} are the effect terms of temperature, strain rate, and DO, respectively. In Eq. 3d, the abbreviation NWC, HWC, and BWR means normal water chemistry, hydrogen water chemistry, and boiling water reactor, respectively. Fig. 1 shows the estimated environmental correction factor of Ni-base alloys using the NUREG/CR-6909 model. It is clearly shown that the value of the environmental correction factor is high when the given temperature is high, strain rate is low, and DO level is below 0.1 ppm.

Using the ASME fatigue design curve and NUREG/CR-6909 F_{en} model, it is possible to estimate the fatigue life of Ni-base alloy welds in an LWR-water environment (i.e., $N_{f,\mathrm{water}}$) as a function of four input features: 1) strain amplitude, 2) temperature, 3) strain rate, and 4) DO. This fatigue life estimation method is a standard model proposed by the Argonne National Laboratory (ANL). In addition to the ANL model, other fatigue life models have been proposed by other organizations [2,16,17]. Although these models have different parameters to fit their own data, the baseline forms of the models are similar.

The aforementioned fatigue life models (or the fatigue design limit) are relatively simple and easy to use but are deterministic and do not explicitly consider the scatter/uncertainty of the given data. Therefore, most of the deterministic models adopted a conservative margin similar to the ASME fatigue design curve. However, in these deterministic models, it is difficult to quantify

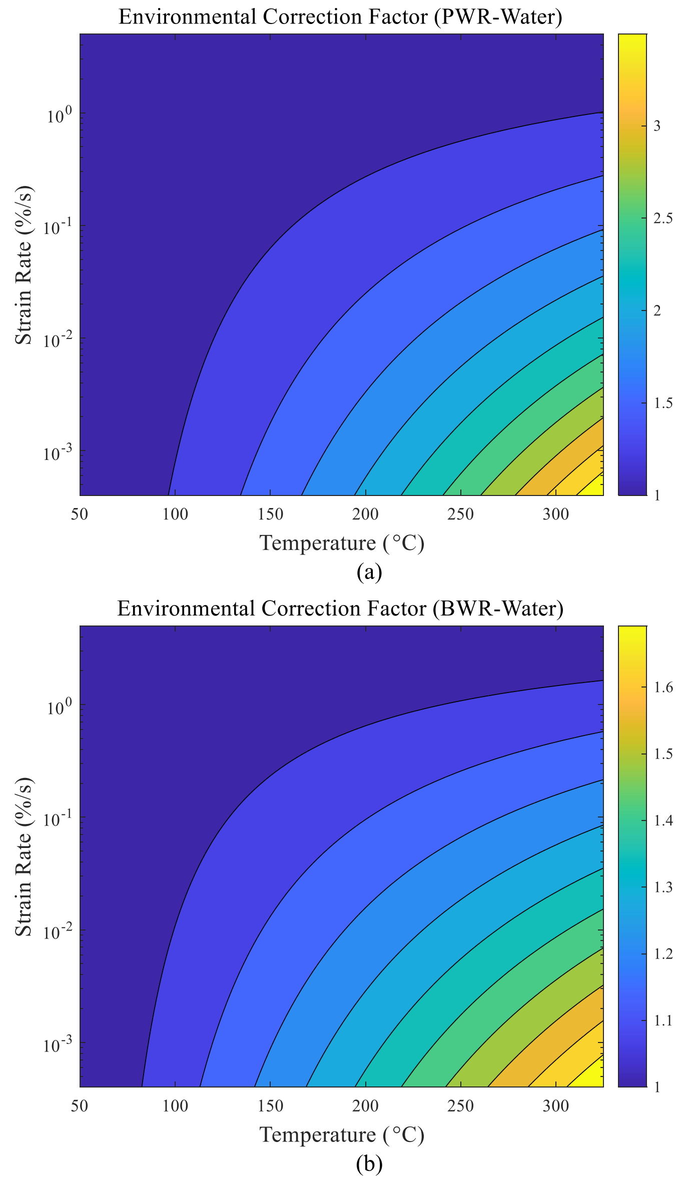

Fig. 1. Estimated environmental correction factor of Ni-base alloys using NUREG/CR-6909 model for a) DO < 0.1 ppm, and b) DO < 0.1 ppm environments.

improved safety with a given conservative margin. This is because, for example, the adoption of a life factor 12 is not equivalent to 12 times of the safety (or reliability) improvement.

To overcome these limitations of the deterministic approach, some studies have developed a probabilistic approach for fatigue life modeling. In general, a probabilistic model has the following advantages: 1) the probabilistic model can quantify the safety margin as a level of failure probability; 2) the probabilistic approach can account for the censored data, which are generally neglected in the deterministic approach; and 3) it is possible to simultaneously consider the multiple feature (e.g., temperature, strain rate/amplitude) effects in the bulk data and statistically optimize the model parameters. Sudret et al. [18,19] proposed a probabilistic framework to assess the fatigue life of NPP components using 304/316 AuSS data. They used the first-order reliability method to compute the probability of failure. However, the proposed model did not consider the environmental effects. Park et al. [20,21] proposed a probabilistic fatigue life model based on the Weibull distribution using in-air and PWR-water 304/316 AuSS data. However, the proposed model did not explicitly model the environmental effects. They estimated two separate probabilistic fatigue models for in-air and PWR-water conditions. Ai et al. [22] estimated the probabilistic fatigue life based on a Weibull distribution. They focused on the notch and size effects on the fatigue life using titanium and aluminum alloy data. Thus, their model also did not consider the environmental effects.

To the best of the authors' knowledge, there is no probabilistic fatigue life model developed for Ni-base alloy welds considering the environmental effects in LWR-water conditions. Therefore, this study aims to conduct statistical analysis on the fatigue data of Ni-base alloys, develop a Weibull-based probabilistic model with a factor that can distinguish the welds from the base metal, and quantify the conservatism of the current fatigue design limit (i.e., ASME design curve + NUREG/CR-6909 F_{en} model) as a level of cumulative failure probability.

2. Available fatigue data of Ni-base alloys

2.1. Fatigue data in NUREG/CR-6909

The NUREG/CR-6909 report aggregated the Ni-base alloy fatigue test data that have been conducted worldwide so far, and the aggregated fatigue data are presented in the S–N plots [1]. In this study, the fatigue test data given in NUREG/CR-6909 were extracted using a graph digitizer software. Table 1 shows the number of extracted fatigue data classified by material grade and testing environment. When classifying the 529 in-air data by base/weld metal, 397 were the base metal data and the remaining 132 were the weld metal data. When classifying the 138 LWR-water data by base/weld metal, 83 were the base metal data and the remaining 55 were the weld metal data.

Fig. 2 shows the S–N plot of the extracted fatigue data. The 529 in-air data consisted of the 522 complete (i.e., failed at that cycle) data and seven right-censored (i.e., surviving at the end of the test) data. The 138 LWR-water data consisted of 132 complete data points and six right-censored data. The solid gray line in Fig. 2 is the reference model that corresponds to the in-air best-fit curve of the AuSS (Eq. 1) [1]. The dashed gray line is the ASME design curve estimated from the in-air best-fit curve using an adjustment life factor of 12 and a stress/strain factor of 2. It is shown that the ASME design curve is not conservative for some Ni-base alloy fatigue data tested in an LWR-water environment. As shown in Fig. 2, the current ASME design curve appears too conservative with respect to the fatigue life of Alloy 718. Therefore, although there is no Alloy 718 data tested in LWR-water condition (see Table 1 and Fig. 2), the NUREG/CR-6909 recommended not to use F_{en} for Alloy 718, even in

Table 1
Number of extracted NUREG/CR-6909 fatigue data classified by material grade, and testing environment.

	Grade	In-air	LWR-water
Base.	A600	176	66
	A690	13	17
	A718	185	-
	A800	23	-
Subtotal.		397	83
Weld.	A62	10	-
	A82	50	8
	A132	6	9
	A152	6	11
	A182	26	26
	A690	6	1
	Other	28	-
Subtotal.		132	55
Total.		529	138

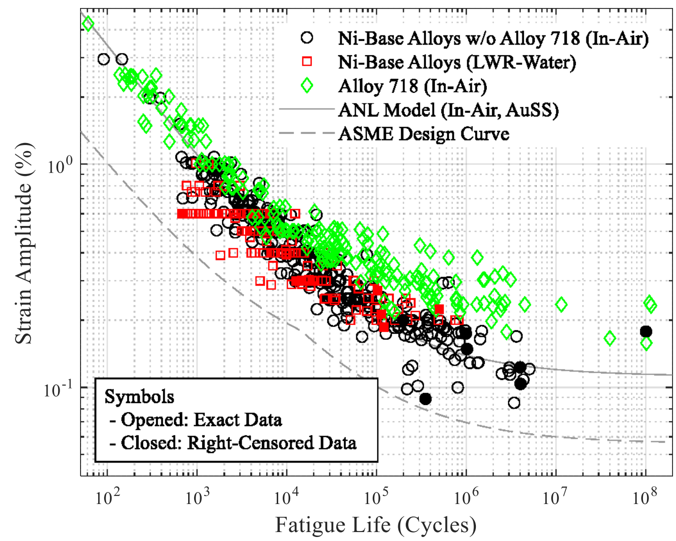

Fig. 2. S–N plot of fatigue data extracted from NUREG/CR-6909.

LWR-water conditions [1]. The numbers of PWR-water and BWR-water data were 65 and 73, respectively. The testing temperature and strain rate of the LWR-water data ranged from $100 \le T \le 325$ °C and $0.001 \le \dot{\varepsilon} \le 0.4\%/s$, respectively.

2.2. New fatigue data of alloy 52M/152 and 82/182

Because either a limited amount of data is available or no data are available, especially for 52M, additional fatigue testing with Ni-base alloy welds has been conducted by the authors for Alloy 52M/152 [23] and Alloy 82/182 [5,24,25]. The new fatigue data of Alloy 52M/152 and 82/182 are summarized in Tables 2 and 3, respectively. A total of 37 (i.e., 27 tests with Alloy 52M/152 and 10 tests with Alloy 82/182) uniaxial strain-controlled fatigue tests ($R = -1$) were performed. The fatigue failure criterion was a 25% tensile load drop according to the American Society for Testing and Materials (ASTM) E606-04 standard [26].

Fig. 3 shows the S–N plot of the new fatigue data of Alloy 52M/152 and 82/182 compared with the fatigue data in NUREG/CR-6909. In Fig. 3, the fatigue data of Alloy 718 were excluded because of its superior fatigue resistance compared to the other Ni-base alloys (see Fig. 2). From Fig. 3, it is likely that there is no remarkable difference in the fatigue lives of the existing and new fatigue data (except joint specimen data, which need substantial number of additional data points both under in-air and water conditions to ascertain the behavior). Therefore, we merged the existing and new fatigue data and treated them as a single database for the development of the probabilistic fatigue life model.

3. Model development

3.1. Model description

There exists a theorem for the distribution of sample maxima or minima, known as the extremal types theorem [27,28]. The extremal types theorem states that if the lower tail of the parent distribution (i.e., population) is bounded, the distribution of sample minima can be approximated to the Weibull distribution [29] which can be expressed as follows [30]:

Table 2
Summary of new Alloy 52M/152 fatigue data.

Test ID	Material	Environment	Strain Amplitude (%)	Strain rate (%/s)	Fatigue life (cycle)
MAH351-1	Alloy 52M Filler	In-air 300 °C	0.35	0.1	20275
MAH500-1			0.5	0.01	4969
MAH501-1				0.1	2373
MAH501-2					3779
MAH501-3					3831
MAH651-1			0.65		1472
MAH651-2					1367
MPH501-1		PWR-water 300 °C	0.5		3841
MPH501-2					1526
MPH501-3					4206
MPH501-4					4168
MPH501-5					8088
BAH501-1	Alloy 152 Butter	In-air 300 °C			4969
BAH501-2					4543
BAH501-3					955
BAH501-4					2625
BAH501-5					913
BAH701-1			0.7		699
BAH701-2					602
BAH701-3					1624
BPH501-1		PWR-water 300 °C	0.5		5366
JAH501-1	Alloy 52M/152 Joint	In-air 300 °C			1032
JAH501-2					1412
JAH701-1			0.7		701
JAH701-2					832
JPH501-1		PWR-water 300 °C	0.5		1790
JPH501-2					2403

Table 3
Summary of new Alloy 82/182 fatigue data.

Test ID	Material	Environment	Strain Amplitude (%)	Strain rate (%/s)	Fatigue life (Cycle)
ET-F61	Alloy 82	In-air 300 °C	0.6	0.01	1133
EN-F62	Filler	PWR-water 300 °C			842
ET-F59	Alloy 182	In-air 300 °C			2984
ET-F63	Butter		0.5		1335
ET-F64			0.4		10480
ET-F65			0.3		9896
ET-F66	Alloy 82/182		0.6		1169
ET-F67	Joint		0.5		835
ET-F68			0.4		5585
ET-F69			0.3		1036

$$F(x;\beta,\eta) = 1 - \exp\left[-\left(\frac{x}{\eta}\right)^{\beta}\right] \tag{4a}$$

$$f(x;\beta,\eta) = \frac{\beta}{\eta}\left(\frac{x}{\eta}\right)^{\beta-1}\exp\left[-\left(\frac{x}{\eta}\right)^{\beta}\right] \tag{4b}$$

where $x \geq 0$ is the domain variable, $\beta > 0$ is the shape parameter, $\eta > 0$ is the scale parameter, and F and f are the cumulative distribution function (CDF) and probability density function (PDF) of the Weibull distribution, respectively.

When considering the fatigue problem, fatigue can occur anywhere within a specimen (or component). That is, every microscopic scale locations (e.g., grain boundaries in corrosive environment) within the specimen are the candidates for the fatigue failure. In this case, to measure a fatigue life of the specimen is similar to a sampling of the earliest (or minimum) failure time among the all fatigue candidates. Although it is unknown that whether the distribution of the failure time for a single fatigue candidate (i.e., parent distribution) will follow the Weibull distribution or not, however, it is obvious that the distribution of the fatigue life for the specimen (i.e., sample minima distribution) will follow the Weibull distribution if the given specimen size is large enough. This is because the fatigue failure time cannot be a negative value and, therefore, the lower tail of the parent distribution is bounded at zero. Thus, it is reasonable to assume that the distribution of the fatigue life (N_f) is a Weibull distribution (see Eq. 5 for CDF). This is a well-known weakest link theory [20,21,31–35] that justifies the use of the Weibull distribution in the field of predicting failure time or material strength [35–41].

$$F\left(N_f;\beta,\eta\right) = 1 - \exp\left[-\left(\frac{N_f}{\eta}\right)^{\beta}\right] \tag{5}$$

For the probabilistic fatigue life prediction in the S–N type domain, the Weibull scale parameter η can be modeled by various covariates (or input features), as shown in Eq. 6. The current fatigue design limit (i.e., ASME design curve + NUREG/CR-6909 F_{en} model) has four input features: 1) strain amplitude (ε_a), 2) temperature (T), 3) strain rate ($\dot{\varepsilon}$), and 4) DO (O). The functional forms of these four covariate effects were adopted from the existing model forms, as described in Eq. 3; however, the model constants were set as unknown parameters (see Eqs. 6b-6f). The overall formula for the Weibull scale parameter η are as follows:

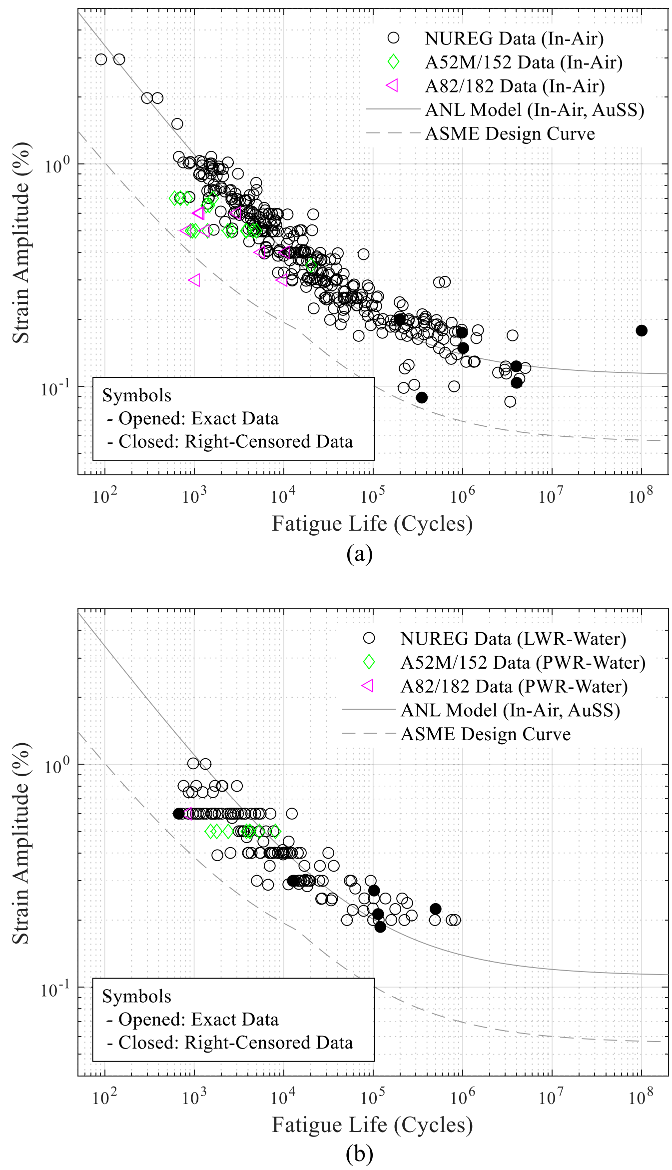

Fig. 3. S–N plot of new fatigue data of Alloy 52M/152 and 82/182, and existing fatigue data except for Alloy 718; (a) in-air, and (b) LWR-water condition.

$$\eta = \frac{\eta_{\text{air,base}}}{F_{\text{en}} F_{\text{weld}}} \tag{6a}$$

$$\eta_{\text{air,base}}(\varepsilon_a; a_{\varepsilon_a}, b_{\varepsilon_a}, c_{\varepsilon_a}) = \left(\frac{\varepsilon_a - c_{\varepsilon_a}}{a_{\varepsilon_a}}\right)^{\frac{1}{b_{\varepsilon_a}}} \tag{6b}$$

$$F_{\text{en}}(T^*, \dot{\varepsilon}^*, O^*) = \begin{cases} 1 & (\text{In} - \text{air}) \\ \exp(-T^* \dot{\varepsilon}^* O^*) & (\text{LWR} - \text{water}) \end{cases} \tag{6c}$$

$$T^*(T; a_T, b_T) = \frac{T - a_T}{b_T} \tag{6d}$$

$$\dot{\varepsilon}^*(\dot{\varepsilon}; a_{\dot{\varepsilon}}) = \ln\left(\frac{\dot{\varepsilon}}{a_{\dot{\varepsilon}}}\right) \tag{6e}$$

$$O^*(\text{DO}) = 1 + (a_{\text{DO}} - 1)H(\text{DO} - 0.1) = \begin{cases} 1 & (\text{PWR or HWC BWR water, DO} < 0.1\ \text{ppm}) \\ a_{\text{DO}} & (\text{NWC BWR water, DO} \geq 0.1\ \text{ppm}) \end{cases} \tag{6f}$$

$$F_{\text{weld}}(\varepsilon_a; a_w, b_w) = \begin{cases} 1 & (\text{Base metal}) \\ a_w \varepsilon_a^{b_w} & (\text{Weld metal}) \end{cases} \tag{6g}$$

where $\eta_{\text{air,base}}$ is the Weibull scale parameter for the base metal in the in-air condition, F_{weld} is the weld correction factor, H is the Heaviside step function, and $a_{\varepsilon_a}, b_{\varepsilon_a}, c_{\varepsilon_a}, a_T, b_T, a_{\dot{\varepsilon}}, a_{\text{DO}}, a_w, b_w$ are the unknown parameters to be estimated using the given fatigue data, as shown in Fig. 3.

In this study, it should be noted that we introduced a new model feature term named weld correction factor (F_{weld}, see Eq. 6g), which enables to consider whether the given material is a base or weld. The reason for introducing the new weld correction factor is that the weld data showed a slightly different behavior from the base metal data, as shown in Fig. 4. It is likely that the overall fatigue life of the weld metal is relatively short compared to that of the base metal when the applied strain amplitude is high. However, when the applied strain amplitude is low, the overall fatigue life of the weld metal is relatively long compared to that of the base metal. This suggests that it would be better to introduce such a modeling feature to reveals the aforementioned characteristics of the weld metal compared with the base metal. In this study, the weld correction factor is assumed to be a power function of the applied strain amplitude to implement the observation shown in Fig. 4.

3.2. Parameter estimation and comparison with current fatigue design limit

In the proposed Weibull-based fatigue model, the total number of model parameters to be estimated is 10 (i.e., β, $a_{\varepsilon_a}, b_{\varepsilon_a}, c_{\varepsilon_a}, a_T, b_T, a_{\dot{\varepsilon}}, a_{\text{DO}}, a_w, b_w$). There are two approaches for the parameter estimation: Frequentist statistics and Bayesian statistics. In a classical way based on Frequentist statistics, the parameters to be estimated are treated as unknown constants and usually estimated by maximum likelihood estimation (MLE) method. The advantage of the MLE method is that the most reliable estimate can be obtained

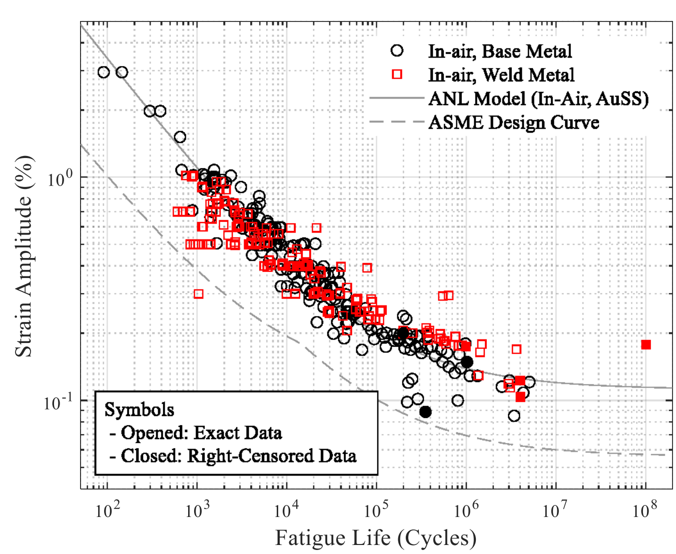

Fig. 4. Available in-air Ni-base alloy base and weld metal fatigue data excluding Alloy 718.

when the number of available data is sufficiently large [42]. The likelihood function for the MLE method can be obtained as follows:

$$L = L_{\mathrm{air}} L_{\mathrm{water}} \tag{7a}$$

$$L_{\mathrm{air}}(\beta, a_{\varepsilon_a}, b_{\varepsilon_a}, c_{\varepsilon_a}) = \prod_{i=1}^{N_{E,\mathrm{air}}} \left[f\left(N_{f,i}, \varepsilon_{a,i}, W\right)\right] \cdot \prod_{j=1}^{N_{R,\mathrm{air}}} \left[1 - F\left(N_{f,j}, \varepsilon_{a,j}, W\right)\right] \tag{7b}$$

$$L_{\mathrm{water}}(\beta, a_{\varepsilon_a}, b_{\varepsilon_a}, c_{\varepsilon_a}, a_T, b_T, a_{\dot{\varepsilon}}, a_{\mathrm{DO}}) = \prod_{i=1}^{N_{E,\mathrm{water}}} \left[f\left(N_{f,i}, \varepsilon_{a,i}, T_i, \dot{\varepsilon}_i, \mathrm{DO}_i, W\right)\right] \cdot \prod_{j=1}^{N_{R,\mathrm{water}}} \left[1 - F\left(N_{f,j}, \varepsilon_{a,j}, T_j, \dot{\varepsilon}_j, \mathrm{DO}_j, W\right)\right] \tag{7c}$$

$$\begin{aligned} l &= \ln L \\ &= \ln L_{\mathrm{air}} + \ln L_{\mathrm{water}} \end{aligned} \tag{7d}$$

where W denotes whether the given material is a base or weld, L is the total likelihood function, L_{air} and L_{water} are the partial likelihood functions for in-air and LWR-water data, respectively, $N_{E,\mathrm{air}}$, $N_{R,\mathrm{air}}$, $N_{E,\mathrm{water}}$, $N_{R,\mathrm{water}}$ are the numbers of complete/right-censored in-air/LWR-water data, i,j are the data indices, and l is the log-likelihood function.

The goal of the MLE is to find a combination of model parameters that maximize the log-likelihood function with the given data. The parameters estimated by MLE are the solutions of the simultaneous differential equations in Eq. 8, which was solved using the numerical methods of the simulated annealing [43] and conjugate gradient [44].

$$\begin{cases} \dfrac{\partial}{\partial \beta} l(\beta, a_{\varepsilon a}, b_{\varepsilon a}, c_{\varepsilon a} a_T, b_T, a_{\varepsilon}, a_{\mathrm{DO}}, a_w, b_w) = 0 \\ \dfrac{\partial}{\partial a_{\varepsilon a}} l(\beta, a_{\varepsilon a}, b_{\varepsilon a}, c_{\varepsilon a} a_T, b_T, a_{\varepsilon}, a_{\mathrm{DO}}, a_w, b_w) = 0 \\ \dfrac{\partial}{\partial b_{\varepsilon a}} l(\beta, a_{\varepsilon a}, b_{\varepsilon a}, c_{\varepsilon a} a_T, b_T, a_{\varepsilon}, a_{\mathrm{DO}}, a_w, b_w) = 0 \\ \dfrac{\partial}{\partial c_{\varepsilon a}} l(\beta, a_{\varepsilon a}, b_{\varepsilon a}, c_{\varepsilon a} a_T, b_T, a_{\varepsilon}, a_{\mathrm{DO}}, a_w, b_w) = 0 \\ \dfrac{\partial}{\partial a_T} l(\beta, a_{\varepsilon a}, b_{\varepsilon a}, c_{\varepsilon a} a_T, b_T, a_{\varepsilon}, a_{\mathrm{DO}}, a_w, b_w) = 0 \\ \dfrac{\partial}{\partial b_T} l(\beta, a_{\varepsilon a}, b_{\varepsilon a}, c_{\varepsilon a} a_T, b_T, a_{\varepsilon}, a_{\mathrm{DO}}, a_w, b_w) = 0 \\ \dfrac{\partial}{\partial a_{\dot{\varepsilon}}} l(\beta, a_{\varepsilon a}, b_{\varepsilon a}, c_{\varepsilon a} a_T, b_T, a_{\varepsilon}, a_{\mathrm{DO}}, a_w, b_w) = 0 \\ \dfrac{\partial}{\partial a_{\mathrm{DO}}} l(\beta, a_{\varepsilon a}, b_{\varepsilon a}, c_{\varepsilon a} a_T, b_T, a_{\varepsilon}, a_{\mathrm{DO}}, a_w, b_w) = 0 \\ \dfrac{\partial}{\partial a_w} l(\beta, a_{\varepsilon a}, b_{\varepsilon a}, c_{\varepsilon a} a_T, b_T, a_{\varepsilon}, a_{\mathrm{DO}}, a_w, b_w) = 0 \\ \dfrac{\partial}{\partial b_w} l(\beta, a_{\varepsilon a}, b_{\varepsilon a}, c_{\varepsilon a} a_T, b_T, a_{\varepsilon}, a_{\mathrm{DO}}, a_w, b_w) = 0 \end{cases} \tag{8}$$

whereas, in the framework of Bayesian statistics, the unknown model parameters are treated as random variables assigned to certain probability distributions. In this study, as well as the aforementioned MLE method, Bayesian inference [45–47] was also carried out to obtain the credible interval of the estimates. With this credible interval, it is possible to interpret that there is a, for example, 95% probability that this interval contains the true value. The detailed procedures of the MLE and Bayesian inference were described in *Supplementary Material*.

Table 4
Comparison of existing fatigue model (i.e., ASME design curve + NUREG/CR-6909 F_{en} model) and estimated Weibull model parameters.

Parameters	Existing model	Weibull model		
		2.5% quantiles	ML estimates	97.5% quantiles
β	n/a	0.980	1.05	1.11
a_{ε_a}	36.2	13.5	16.7	19.8
b_{ε_a}	-0.521	-0.426	-0.406	-0.379
c_{ε_a}	0.112	0.0578	0.0731	0.0807
a_T	50	30.7	50.0	59.2
b_T	1964 (=275/0.14)	1230	1470	2550
$a_{\dot{\varepsilon}}$	5	2.13	4.31	5.90
a_{DO}	0.4285 (=0.06/0.14)	0.0624	0.373	0.879
a_w	n/a	2.42	3.29	4.21
b_w	n/a	1.67	1.96	2.22

Table 4 shows a comparison of the current fatigue design limit model parameters and the estimated Weibull model parameters using the Ni-base alloy fatigue data presented in Fig. 3. In Table 4, 2.5% and 97.5% quantiles are the lower/upper bounds of the 95% credible interval obtained by the Bayesian inference, and ML estimates are the maximum likelihood estimates obtained by the simulated annealing and conjugate gradient methods. It is worth noting that new parameters were added (i.e., β, a_w, b_w), and the Weibull model parameters were slightly different from those of the current design limit model. Table 5 lists the applicable ranges of the estimated Weibull model. The applicable range herein implies the data range used for estimating the Weibull model.

Fig. 5 shows the Weibull model with the ML estimates in Table 4 under the in-air condition for the base and weld metals. In Fig. 5, the red line is the Weibull scale parameter line, which implies a 63.2% cumulative failure probability, and the red shaded area represents the 95% confidence interval of the fatigue life estimates (i.e., from 2.5% to 97.5%). This capability of the probabilistic approach to provide a failure probability for the fatigue life is the most significant benefit, which enables the quantification of the safety margin as a level of the failure probability. As expected, Fig. 5 shows that the estimated fatigue life of the weld metal was longer at the low strain amplitude (and shorter at the high strain amplitude) compared with that of the base metal, which was revealed by introducing the weld correction factor F_{weld}.

Fig. 6 shows the estimated environmental correction factor of the Ni-base alloys in the Weibull distribution model. The inside of the white dashed box represents the applicable range of the model (see Table 5). Similar to the NUREG/CR-6909 F_{en} model (see Fig. 1), the Weibull model also predicts high value of the environmental correction factor when the given temperature is high, strain rate is low, and DO level is below 0.1 ppm.

Fig. 7 shows the ratio of the environmental correction factors between the NUREG/CR-6909 and Weibull models (i.e., $F_{\mathrm{en,Weib}}/F_{\mathrm{en,NUREG}}$). It is shown that the Weibull model always estimates a larger than the NUREG/CR-6909 model in the applicable range. The ratio of between two models can reach up to 1.4 when the temperature is high, strain rate is low, and the DO is less than 0.1 ppm (see Fig. 7a).

In Figs. 8 and 9, the predicted fatigue lives are compared with the measured values for the base and weld metals, respectively. In

Table 5
Applicable range of Weibull distribution model.

Input features	Model Applicable range
Strain amplitude	$0.0852 < \varepsilon_a < 2.95$ (%)
Temperature	$100 \le T \le 325$ (°C)
Strain rate	$0.001 \le \dot{\varepsilon} \le 0.4$ (%/s)
Dissolved oxygen concentration	$0.005 \le O \le 8.0$ (ppm)
Material	Ni-base alloy base and weld metals except Alloy 718

the figures, the solid black line indicates the 1:1 correlation line. Fig. 8a (for the base metal) and 9a (for the weld metal) show the cases when the predicted fatigue life is calculated using the current fatigue design limit model (i.e., ASME design curve + NUREG/CR-6909 F_{en} model). Whereas Fig. 8b–d (for the base metal) and 9b-9d (for the weld metal) show the cases when the predicted fatigue life is calculated using the Weibull distribution model with cumulative failure probabilities of 50%, 2.5%, and 1%, respectively. Because the Weibull distribution is a probabilistic model, it is necessary to set a certain level of failure probability to estimate the fatigue life. In this case, the 50% probability implies the best estimates, and the 2.5% (or 1%) probability implies the conservative estimates. This is because the 50% probability is a middle of the confidence interval of the fatigue life estimates (i.e., unbiased median), and 2.5% (or 1%) probability is a lower tail of the confidence interval (i.e., conservative lower bound). Figs. 8b and 9b show that most of the fatigue life estimates are distributed near the 1:1 correlation line. Therefore, it is concluded that the Weibull model reasonably fits all the in-air/LWR-water data well. Based on the comparison of Fig. 8a and d or 9a and 9d, the overall margin in the current fatigue design limit model is similar to the margin of the Weibull model with 2.5% of the cumulative failure probability. This potentially implies that the inherent safety margin in the current fatigue design limit model is approximately 2.5% of the failure probability. However, it should be noted that the margin in the current fatigue design limit model is

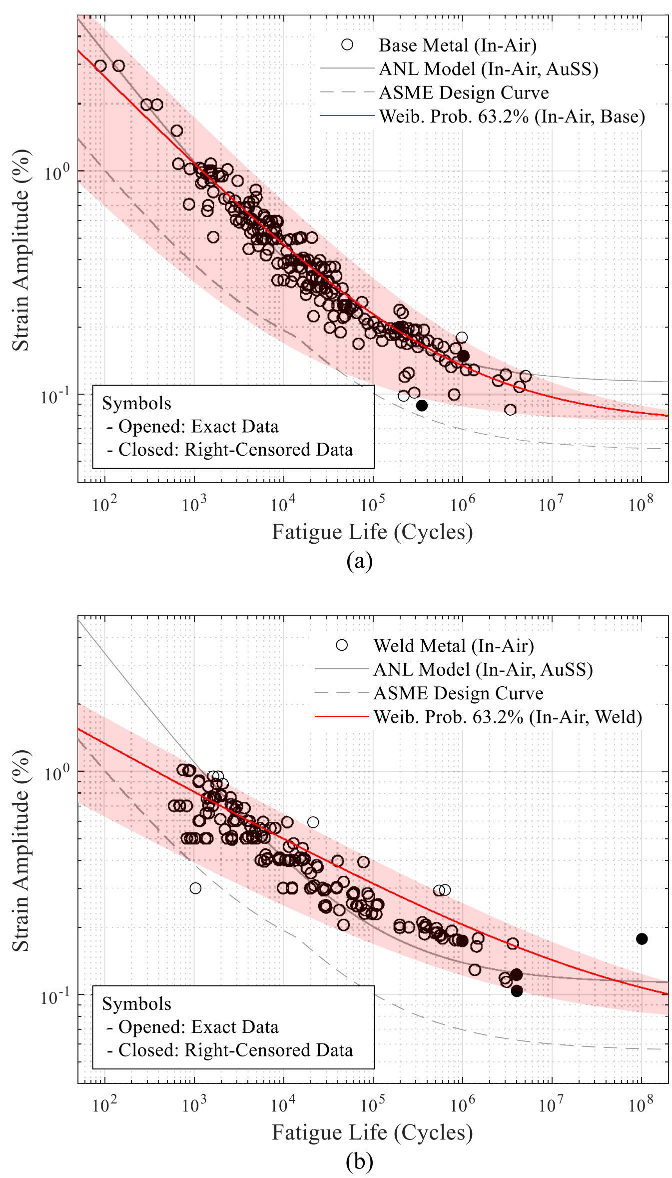

Fig. 5. Comparison of fatigue data, ASME design curve, and Weibull model at in-air condition for (a) base, and (b) weld metal data (red shades: 95% confidence interval).

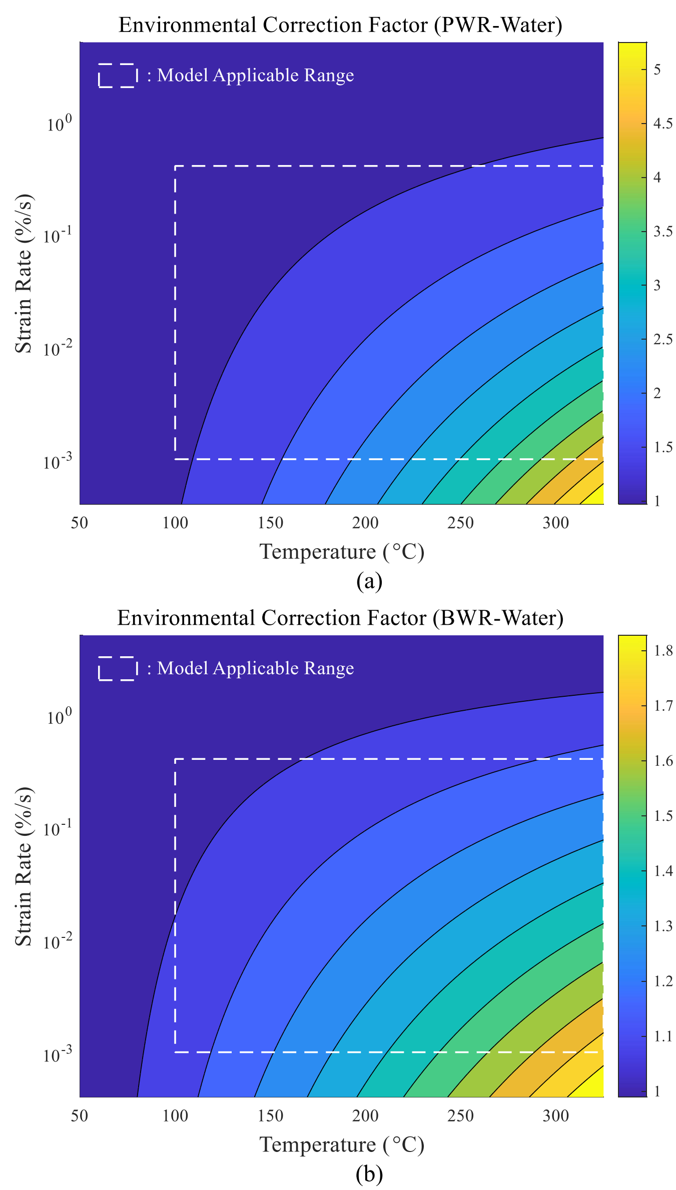

Fig. 6. Estimated environmental correction factor of Ni-base alloys using Weibull model for a) DO < 0.1 ppm, and b) DO < 0.1 ppm conditions.

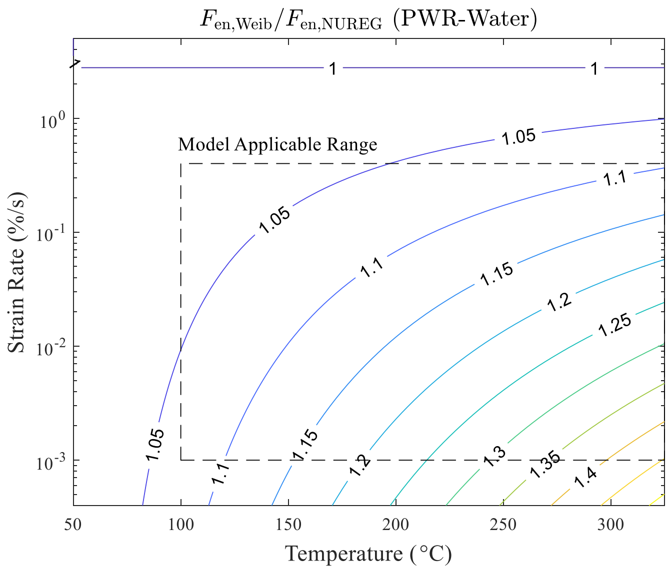

(a)

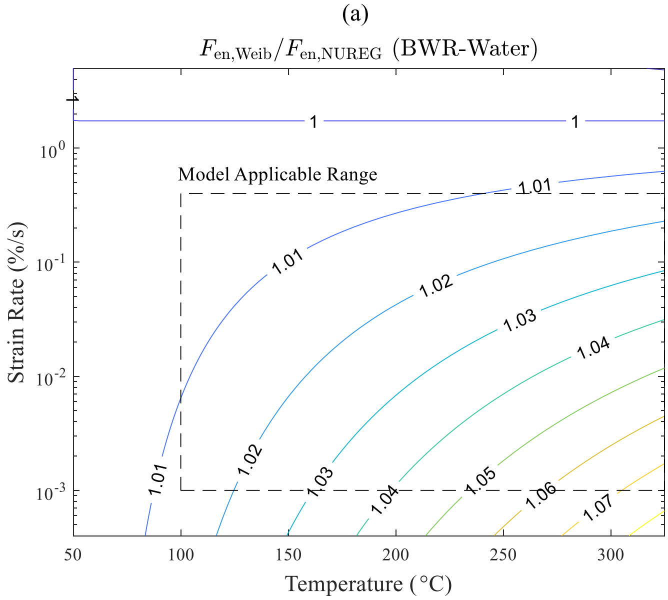

(b)

Fig. 7. Ratio of environmental correction factor between Weibull distribution and NUREG/CR-6909 models for (a) DO < 0.1 ppm, and b) DO < 0.1 ppm conditions.

inconsistent with the weld metal data (see Fig. 9a). That is, the margin is too large for some long-survived data and too small for some early-failed data. However, the Weibull model shows a consistent margin over the entire failure cycle range of interest (see Fig. 9c and d).

3.3. Discussion

The different/improved points of the Weibull distribution model compared with the current fatigue design limit model (i.e., ASME design curve + NUREG/CR-6909 F_{en} model) are as follows:

1) The current fatigue design limit model determines the fatigue life in a deterministic manner. Therefore, it is difficult to quantify improved safety (or reliability) by adopting a conservative margin. However, the Weibull distribution model estimates the fatigue life in a probabilistic manner, which enables one to easily quantify the improved safety (or reliability) based on the level of failure probability.
2) In most deterministic fatigue life estimation approaches, right-censored (or non-failed) data were neglected. However, the Weibull model used both complete and right-censored fatigue data to estimate the fatigue life.
3) The current fatigue design limit model used only a small amount of screened data when estimating each covariate-effect model. For example, when estimating the effect of the strain rate, the NUREG/CR-6909 F_{en} model used only a small amount of the screened data satisfying the condition that the other features (e.g., temperature, strain amplitude, etc.) are the same, except for the strain rate [1]. However, the Weibull model uses all bulk data to estimate all the feature effect models through the MLE method. Therefore, the resulting model parameters are statistically optimized.
4) The current fatigue design limit model does not consider whether the given material is a base or weld. However, the developed Weibull model can consider this feature by adopting the weld correction factor, which enables the Weibull model to reveal the different fatigue characteristics of Ni-base alloy welds from the base alloy.

As shown in Fig. 5, the fatigue life of the weld metal under air conditions was longer than that of the base metal when the applied strain amplitude was relatively low. However, when the applied strain amplitude was relatively high, the fatigue life of the weld metal appeared to be shorter than that of the base metal. This may be due to the higher yield strength and residual stress of the welds, which limits the plastic deformation of the material at low applied strain amplitude, and accelerate the fatigue crack propagation at high applied strain amplitude. Further testing and research are necessary to confirm the difference in the fatigue characteristics between the base and weld metals for (both the homogeneous and joint welds) Ni-base alloys.

If the fatigue characteristics of the base and weld metals for Ni-base alloys are different, the fatigue failure location of a component consisting of both the base and weld metal (e.g., nozzles connected to the reactor pressure vessel head or bottom) may depend on the applied strain amplitude. For example, if the applied strain amplitude is relatively high, the weld may become more vulnerable to fatigue damage, whereas if a relatively low strain amplitude is applied, the base may become so. Therefore, when using the Weibull distribution model, the fatigue life of the component should be conservatively estimated by considering the applied strain amplitude. Similarly, for the heat-affected zone, which is difficult to classify as either base or weld, it appears reasonable to predict the fatigue life conservatively similar to the aforementioned case.

As shown in Fig. 9, the margin in the current fatigue design limit model is inconsistent for the Ni-base alloy weld data. However, the Weibull model showed a consistent margin. Therefore, the use of the Weibull model might mitigate the excessive safety margin exhibited in the current fatigue design limit model. In addition, users of the Weibull model can select any level of failure probability in advance, which enables the determination of the conservativeness of the model for the fatigue life prediction. When considering next-generation reactors such as small modular reactors, particularly allowing the load-following operation, the use of the Weibull model (or any other probabilistic model) may become essential for the fatigue design because the load-following operation can make it difficult for new reactors to satisfy the current fatigue design limit. Therefore, the Weibull model can be a new method for systematically mitigating excessive margins.

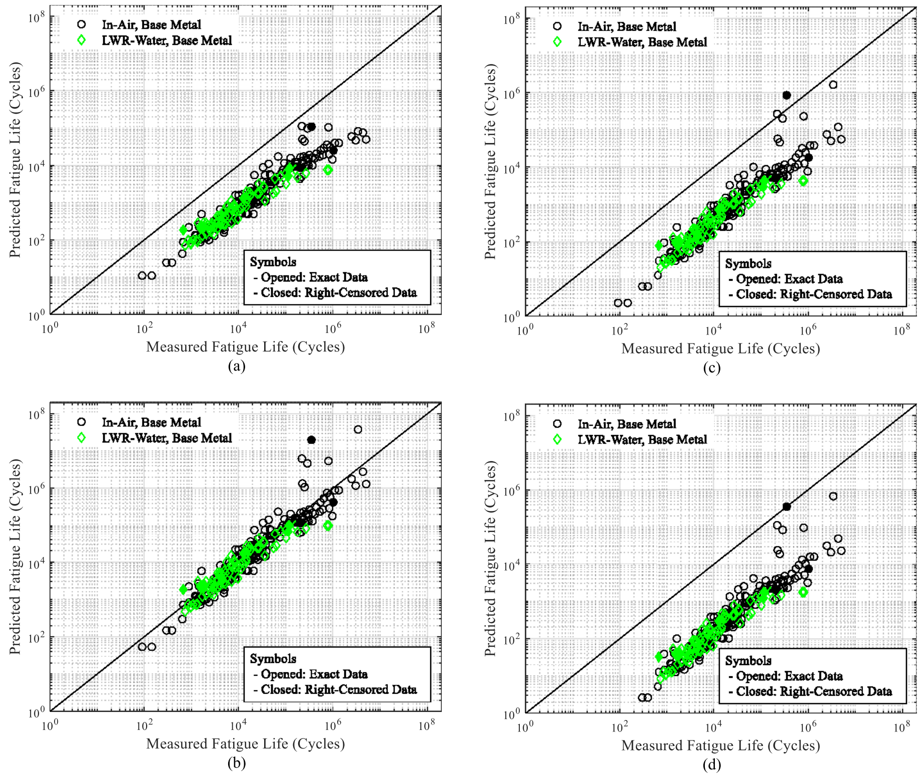

Fig. 8. Measured vs. predicted fatigue life of base metal when applying (a) current fatigue design limit, Weibull model with probability of (b) 50%, (c) 2.5%, and (d) 1%.

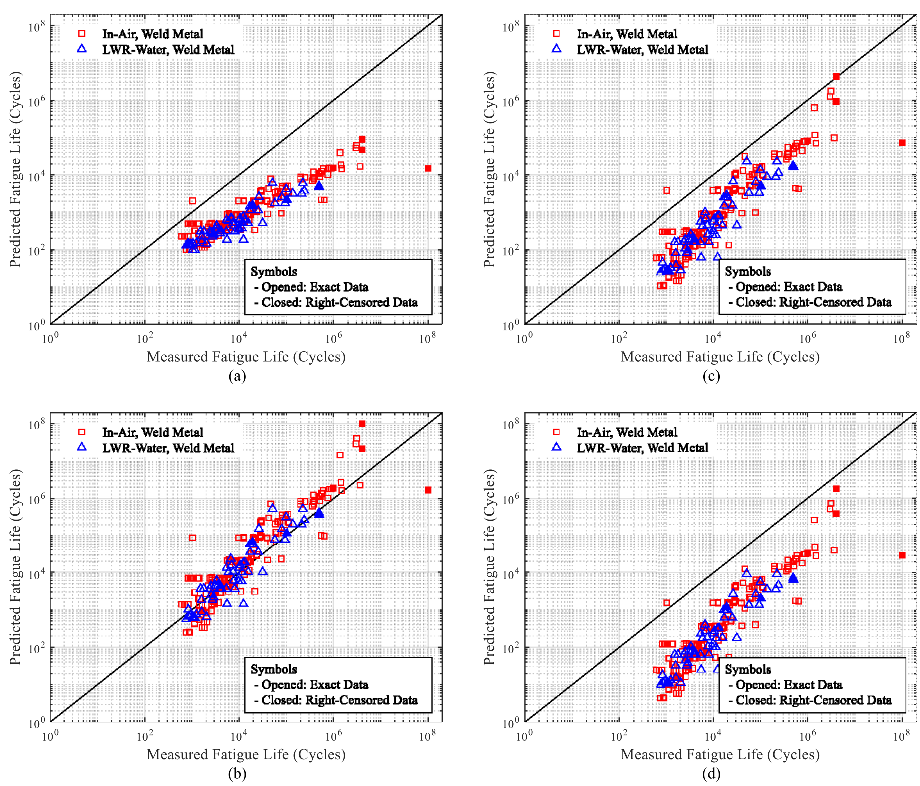

Fig. 9. Measured vs. predicted fatigue life of weld metal when applying (a) current fatigue design limit, Weibull model with probability of (b) 50%, (c) 2.5%, and (d) 1%.

4. Conclusions

Conducting statistical analysis of the fatigue data in NUREG/CR-6909, except for Alloy 718, and the new fatigue data of Alloy 52M/152 and 82/182, led to the development of the probabilistic fatigue life model for Ni-base alloys, which was based on the Weibull distribution. The developed Weibull model can consider right-censored data (i.e., non-failed data) and quantify the improved safety (or reliability) based on the level of failure probability. The following conclusions were drawn:

- The Weibull model always estimates a larger than the NUREG/CR-6909 model in the model applicable range. The ratio of between two models can reach up to 1.4 when the temperature is high, strain rate is low, and the DO is less than 0.1 ppm.
- By introducing the weld correction factor, the developed Weibull model was able to reveal the differences in the fatigue characteristics between the base and weld metals for Ni-base alloys. The estimated fatigue life of the weld metal was longer at the low strain amplitude (and shorter at the high strain amplitude) compared with that of the base metal presumably because of the higher yield strength and residual stress.
- The overall margin in the current fatigue design limit model (ASME design curve + NUREG/CR-6909 F_{en} model) is similar to that of the Weibull model with a cumulative failure probability of approximately 2.5%.
- The margin in the current fatigue design limit model was inconsistent with the weld metal data. However, the Weibull model showed a consistent margin over the entire failure cycle range.

Declaration of competing interest

The authors declare that they have no known competing financial interests or personal relationships that could have appeared to influence the work reported in this paper.

Acknowledgement

This work was supported by the National Research Foundation of Korea (NRF) grant funded by the Korean government (MSIT: Ministry of Science and ICT) (No. 2019M2A8A100064013) and also supported by the Korea Institute of Energy Technology Evaluation and Planning (KETEP) and the Ministry of Trade, Industry & Energy (MOTIE) of the Republic of Korea (No. 20214000000410). Part of the reported work was also supported through INERI and U.S. Department of Energy's Light Water Reactor Sustainability program under the work package of environmental fatigue study.

Part of the reported work has been created by UChicago Argonne, LLC, Operator of Argonne National Laboratory ("Argonne"). Argonne, a U.S. Department of Energy Office of Science laboratory, is operated under Contract No. DE-AC02-06CH11357. The U.S. Government retains for itself, and others acting on its behalf, a paid-up nonexclusive, irrevocable worldwide license in said article to reproduce, prepare derivative works, distribute copies to the public, and perform publicly and display publicly, by or on behalf of the Government.

Appendix A. Supplementary data

Supplementary data to this article can be found online at https://doi.org/10.1016/j.net.2022.08.005.

References

[1] O.K. Chopra, G.L. Stevens, Effect of LWR Water Environments on the Fatigue Life of Reactor Materials (NUREG/CR-6909, Rev. 1), United States Nuclear Regulatory Commission, Office of Nuclear Regulatory, 2018.
[2] J. Gao, C. Liu, J. Tan, Z. Zhang, X. Wu, E.H. Han, R. Shen, B. Wang, W. Ke, Environmental fatigue correction factor model for domestic nuclear-grade low-alloy steel, Nuclear Engineering and Technology 53 (2021) 2600–2609, https://doi.org/10.1016/J.NET.2021.02.014.
[3] ASME, Rules for Construction on Nuclear Facility Components: Supports. III. Division 1-Subsection NF, American Society of Mechanical Engineers, 2013.
[4] M. Benson, D. Rudland, A. Csontos, Weld Residual Stress Finite Element Analysis Validation: Part 1 – Data Development Effort (NUREG-2162), 2014.
[5] S. Mohanty, J. Listwan, S. Majumdar, K. Natesan, Tensile behavior of 82/182 filler, butter and heat-affected-zones in a 508 LAS-316 SS dissimilar weld: tensile test, material model and finite element model validation, in: Pressure Vessels and Piping Conference, American Society of Mechanical Engineers, 2019, V001T01A024.
[6] H.P. Seifert, S. Ritter, H.J. Leber, Corrosion fatigue crack growth behaviour of austenitic stainless steels under light water reactor conditions, Corrosion Science 55 (2012) 61–75.
[7] H.P. Seifert, S. Ritter, H.J. Leber, Corrosion fatigue initiation and short crack growth behaviour of austenitic stainless steels under light water reactor conditions, Corros Sci 59 (2012) 20–34.
[8] H.P. Seifert, S. Ritter, H. Leber, Effect of static load hold periods on the corrosion fatigue behavior of austenitic stainless steels in simulated BWR environments, in: Proceedings of the 15th International Conference on Environmental Degradation of Materials in Nuclear Power Systems—Water Reactors, Springer, 2011, pp. 547–560.
[9] C. Jang, P.-Y. Cho, M. Kim, S.-J. Oh, J.-S. Yang, Effects of microstructure and residual stress on fatigue crack growth of stainless steel narrow gap welds, Materials & Design 31 (2010) 1862–1870.
[10] H. Cho, B.K. Kim, I.S. Kim, C. Jang, D.Y. Jung, Fatigue life and crack growth mechanisms of the type 316LN austenitic stainless steel in 310° C deoxygenated water, J Nucl Sci Technol 44 (2007) 1007–1014.
[11] H. Cho, B.K. Kim, I.S. Kim, C. Jang, Low cycle fatigue behaviors of type 316LN austenitic stainless steel in 310° C deaerated water–fatigue life and dislocation structure development, Materials Science and Engineering: A 476 (2008) 248–256.
[12] J.-D. Hong, J. Lee, C. Jang, T.S. Kim, Low cycle fatigue behavior of alloy 690 in simulated PWR water—effects of dynamic strain aging and hydrogen, Materials Science and Engineering: A 611 (2014) 37–44.
[13] S. Xu, X.Q. Wu, E.H. Han, W. Ke, Y. Katada, Crack initiation mechanisms for low cycle fatigue of type 316Ti stainless steel in high temperature water, Materials Science and Engineering: A 490 (2008) 16–25.
[14] X. Wu, Y. Katada, Strain-rate dependence of low cycle fatigue behavior in a simulated BWR environment, Corros Sci 47 (2005) 1415–1428.
[15] U.S.N.R. Commission, Guidelines for evaluating the effects of light-water reactor water environments in fatigue analysis of metal components, Regulatory Guide 1 (2018).
[16] Environmental Fatigue Evaluation Method for Nuclear Power Plants, JNES-SS-1005), 2011.
[17] C. Faidy, Status of French road map to improve environmental fatigue rules, in: Pressure Vessels and Piping Conference, Citeseer, 2012, pp. 567–573.
[18] B. Sudret, Z. Guédé, Probabilistic assessment of thermal fatigue in nuclear components, Nuclear Engineering and Design 235 (2005) 1819–1835.
[19] B. Sudret, P. Hornet, J.-M. Stephan, Z. Guede, M. Lemaire, Probabilistic assessment of fatigue life including statistical uncertainties in the SN curve, in: 17th International Conference on Structural Mechanics in Reactor Technology (SMiRT 17)), 2003, pp. 2803–2811. Prague, Czech Republic.
[20] J.P. Park, S. Mohanty, C.B. Bahn, S. Majumdar, K. Natesan, Weibull and bootstrap-based data-analytics framework for fatigue life prognosis of the pressurized water nuclear reactor component under harsh reactor coolant environment, Journal of Nondestructive Evaluation, Diagnostics and Prognostics of Engineering Systems 3 (2020).
[21] J.P. Park, S. Mohanty, C.B. Bahn, Weibull and bootstrap based probabilistic fatigue life modeling of stainless steel under PWR coolant water environment condition, in: 19th International Conference on Environmental Degradation of Materials in Nuclear Power Systems - Water Reactors, 2019, pp. 1036–1042. Boston, USA.
[22] Y. Ai, S.-P. Zhu, D. Liao, Probabilistic modelling of notch and size effect of components under fatigue loadings, Procedia Structural Integrity 22 (2019) 70–77.
[23] J. Ham, S.C. Yoo, Y. Lee, D. Park, J.H. Kim, Low cycle fatigue life of alloy 52M weld metal in simulated PWR environment, in: Transactions of the Korean Nuclear Society Virtual Spring Meeting, Korean Nuclear Society, 2021.
[24] S. Mohanty, W. Soppet, S. Majumdar, K. Natesan, Tensile and Fatigue Testing and Material Hardening Model Development for 508 LAS Base Metal and 316 SS Similar Metal Weld under In-Air and PWR Primary Loop Water Conditions (ANL/LWRS-15/02), Argonne National Lab.(ANL), Argonne, IL (United States), IL, USA, 2015.
[25] S. Mohanty, J. Listwan, Development of Digital Twin Predictive Model for PWR Components: Updates on Multi Times Series Temperature Prediction Using Recurrent Neural Network, DMW Fatigue Tests, System Level Thermal-

Mechanical-Stress Analysis (ANL/LWRS-21/02), Argonne National Lab.(ANL), Argonne, IL (United States), 2021.
[26] ASTM International, Standard Practice for Strain-Controlled Fatigue Testing, ASTM, 2017. E606-04).
[27] B.V. Gnedenko, On a local limit theorem of the theory of probability, Uspekhi Matematicheskikh Nauk 3 (1948) 187–194.
[28] R.A. Fisher, L.H.C. Tippett, Limiting forms of the frequency distribution of the largest or smallest member of a sample, in: Mathematical Proceedings of the Cambridge Philosophical Society, Cambridge University Press, 1928, pp. 180–190.
[29] R.L. Wolpert, Extremes, Department of Statistical Science, Duke University, 2014. https://www2.stat.duke.edu/courses/Fall15/sta711/lec/topics/extremes.pdf. (Accessed 15 December 2021). accessed.
[30] W. Weibull, Wide applicability, J Appl Mech 103 (1951) 293–297.
[31] J.P. Park, C.B. Bahn, Uncertainty evaluation of weibull estimators through Monte Carlo simulation: applications for crack initiation testing, Materials 9 (2016), https://doi.org/10.3390/ma9070521.
[32] J.P. Park, C. Park, J. Cho, C.B. Bahn, Effects of cracking test conditions on estimation uncertainty for weibull parameters considering time-dependent censoring interval, Materials 10 (2017), https://doi.org/10.3390/ma10010003.
[33] J.P. Park, C. Park, Y.-J. Oh, J.H. Kim, C.B. Bahn, Statistical analysis of parameter estimation of a probabilistic crack initiation model for Alloy 182 weld considering right-censored data and the covariate effect, Nuclear Engineering and Technology (2018) 50, https://doi.org/10.1016/j.net.2017.09.005.
[34] J.I. McCool, Using the Weibull Distribution: Reliability, Modeling, and Inference, John Wiley & Sons, 2012.
[35] Z.P. Bazant, J.-L. Le, Probabilistic Mechanics of Quasibrittle Structures: Strength, Lifetime, and Size Effect, Cambridge University Press, 2017.
[36] M.H. Abdallah, E.M. Abdin, A.I. Selmy, U.A. Khashaba, Reliability Analysis of GFRP Pultruded Composite Rods, International Journal of Quality & Reliability Management, 1996.
[37] U.A. Khashaba, Fatigue and reliability analysis of unidirectional GFRP composites under rotating bending loads, J Compos Mater 37 (2003) 317–331.
[38] R. Sakin, I. Ay, Statistical analysis of bending fatigue life data using Weibull distribution in glass-fiber reinforced polyester composites, Materials & Design 29 (2008) 1170–1181.
[39] M. Goto, Statistical investigation of the behaviour of small cracks and fatigue life in carbon steels with different ferrite grain sizes, Fatigue & Fracture of Engineering Materials & Structures 17 (1994) 635–649.
[40] M.S. Kumar, S. Vijayarangan, Analytical and experimental studies on fatigue life prediction of steel and composite multi-leaf spring for light passenger vehicles using life data analysis, Materials Science 13 (2007) 141–146.
[41] L.M. Leemis, Reliability: Probabilistic Models and Statistical Methods, Prentice-Hall, Inc., 1995.
[42] U. Genschel, W.Q. Meeker, A comparison of maximum likelihood and median-rank regression for Weibull estimation, Quality Engineering 22 (2010) 236–255.
[43] D. Bertsimas, J. Tsitsiklis, Simulated annealing, Statistical Science 8 (1993) 10–15.
[44] S.S. Rao, Engineering Optimization: Theory and Practice, John Wiley & Sons, 2019.
[45] Y. Liu, A.I. Abeyratne, Practical Applications of Bayesian Reliability, John Wiley & Sons, 2019.
[46] J.F. Lawless, Statistical Models and Methods for Lifetime Data, John Wiley & Sons, 2011.
[47] D.F. Falaakh, C.B. Bahn, Bayesian approach for prediction of primary water stress corrosion cracking in Alloy 690 steam generator tubing, Nuclear Engineering and Technology (2022).